CARMA Memorandum Series #49

Single–Dish Aperture Efficiency Measurements at CARMA

Stephen M. White

Univ. of Maryland

B. Ashley Zauderer

Univ. of Maryland

March 13, 2009

ABSTRACT

We describe the process by which single dish aperture efficiency measurements are carried out for the antennas of the CARMA array. The basis for the measurements is explained and the practical details are described. Related topics such as the approximations used at CARMA to calculate atmospheric opacity from weather data, the analysis of sky dips to actually measure atmospheric opacity, the model for lunar brightness temperature and effective primary beam sizes are also discussed.

Change Record

Revision	Date	Author	Sections/Pages Affected
	Remarks		
1.1	2008-Aug-04	SMW/BAZ	1-5
	Draft memo		
1.2	2008-Aug-24	SMW/BAZ	1-5
	Reorganized after comments from James		
2.0	2009-Mar-05	SMW/BAZ	1-5
	Updated dip and measured values sections		

1. Introduction

The *aperture efficiency* of an antenna is simply the ratio of the effective collecting area (in terms of collected power that gets into the receiver feed horn) to the physical collecting area. An ideal antenna would have 100% efficiency. However, numerous factors can absorb the incident radiation or scatter it out of the beam path, e.g.,

- blockage of the dish surface by the subreflector and the support legs;

- gaps between the individual panels that typically make up the reflecting surface of millimeter dishes, and poor reflection from the heads of the screws used to mount the panels;

- deviation of the dish shape from a parabola such that the incident radiation is not all collected at the focus (spillover, taper). This property often changes with dish elevation as the orientation of gravitational forces relative to the support structure changes and the dish deforms;

- imperfect illumination of the subreflector and then the feed horn by the aperture. In order to reduce spillover the illumination pattern is often deliberately tapered at the edge of the aperture. This and any unintentional imperfections in the illumination pattern will reduce aperture efficiency;

- diffraction at the edge of the subreflector;

- incorrect focus position (either lateral or axial) for the subreflector; and

- imperfect reflection due to roughness on the dish surface (referred to as "Ruze loss").

A thorough description of the elements that control aperture efficiency for reflecting antennas is given by Baars (2003). All these effects can each contribute losses of several percent in efficiency, and since they combine in series (i.e., geometrically), they can add up to tens of percent loss in efficiency compared to an ideal antenna. Lugten (1995) discusses the efficiency of the BIMA 6.1m antennas: estimates of the above effects lead to a theoretical estimate of 75% for the main beam aperture efficiency, and measurements at Hat Creek were consistent with this result. This is regarded as good for a millimeter–wavelength telescope.

There are several ways to measure the aperture efficiency. Here we discuss the use of single–dish total power measurements (a separate memo discusses interferometric measurements at CARMA). The discussion is written from a non–expert's point of view, based on a number of sources, including the basic paper on calibration by Ulich & Haas (1976), the NRAO 12m telescope manual (Folkers 2004), the HIFI/Herschel calibration document (Kramer 2005), ALMA calibration documents (Mangum 2002; Moreno & Guilloteau 2002), and Dave Woody's CARMA calibration memo (Woody 2006).

2. Single–dish aperture efficiency measurements: Theory

The aperture efficiency of a dish may be determined from measurements of the power in the receiver when illuminated by three different targets: blank sky, a bright planet, and an ambient-temperature load. A source

such as a planet or a maser typically only fills a small fraction of the telescope beam, and thus is appropriate to measure the "main–beam" aperture efficiency ε relevant to interferometer observations.

We will discuss single–dish power measurements along the lines of the framework used in the CARMA memo on T_{sys} calculation (Woody 2006). First consider the contributions to the receiver power when the telescope points at blank sky. The power measured at the receiver is the product of a gain G (e.g., in units of dB per Kelvin) with the following temperature contributions:

- The intrinsic thermal noise of the receiver, T_{rec}.

- The thermal emission of the optically thin atmosphere above the telescope: we represent the atmosphere by a single temperature T_{atm} and an opacity τ (which, for a given telescope elevation El, is the zenith opacity τ_0 times the "air mass" $1/\sin(El)$), so that the atmospheric contribution is $T_{atm}\left(1-e^{-\tau}\right)$.

- Above the atmosphere, the sky is filled by the cosmic microwave background (CMB). This must pass through the atmosphere and hence is attenuated by a factor $e^{-\tau}$ when it reaches the telescope.

- The subreflector support legs and any illumination into the feed from optical paths that do not reflect from the dish, such as beyond the edges of the dish ("rear spillover") or the edge of the subreflector ("forward spillover"), contribute to the measured power.

Although we use temperatures in the formulae presented here, in each case the relevant value to use is the Rayleigh–Jeans curve equivalent contribution, $J(\nu,T) = (h\nu/k_B)/(\exp(h\nu/k_BT)-1)$. For example, the temperature of the CMB is 2.73 K, but the temperature we need at millimeter wavelengths, T_{CMB}, is the Rayleigh–Jeans curve equivalent $J(\nu,2.73) \approx 1$ K at 3 mm wavelength. In the 3 mm window $J(T) \approx T-2$ to quite a good approximation above a few K, and $J(T) \approx T-5$ in the 1.3 mm window, so the difference between T and $J(T)$ is negligible except for the CMB.

The expression for the power measured on the sky is thus

$$P_{sky} = G\{T_{rec} + (1-e^{-\tau})\eta T_{atm} + (1-\eta)T_{spill} + e^{-\tau}\eta T_{CMB}\} \tag{1}$$

Here η is a "coupling efficiency" that is distinct from the aperture efficiency appropriate to compact cosmic radio sources that we seek to measure. The distinction between different forms of efficiency can be very confusing: Mangum (2002) lists no less than 7 separate types of "telescope efficiency" in his Appendix D. Here η is the efficiency appropriate for the coupling of a source that completely fills the forward hemisphere of the dish with a uniform temperature. In this situation the receiver is effectively enclosed in a black body cavity at the corresponding temperature, and the focussing properties of the aperture have little effect on the temperature seen by the receiver. The only decrements to this efficiency are the small effects of rear spillover, blockage and ohmic losses. The 12m Telescope Manual (Folkers 2004) calls η the "warm spillover efficiency", Serabyn et al. (1998) refer to it as the "coupling efficiency" and Plambeck (2000) describes it as the "spillover efficiency". This efficiency is typically close to unity.

It is common in calibration documents to use the same base symbol η, suitably subscripted, to refer to all forms of telescope efficiency. While experts have no difficulty in keeping track of the seven distinct forms of η, the use of a single symbol tends to cause confusion for the non–expert. To minimize confusion here, we will use different symbols. In this document η will always and only refer to the "spillover" or "coupling" efficiency described above.

Since the CMB and the sky contribution both in effect fill the forward hemisphere of the dish, they are both modified by η. The receiver noise, on the other hand, is intrinsic and thus not affected by the coupling efficiency. T_{spill} is the effective temperature of the rear spillover and blockage effects, whose contribution to the measured power is proportional to $(1 - \eta)$ since it enters the feed through the portion of the aperture that is not illuminated by the forward hemisphere. In most discussions of calibration (e.g., Kutner & Ulich 1981; Folkers 2004) T_{spill} is set equal to the ambient temperature since most of the contributions (ground, subreflector support, etc.) are at that temperature.

As part of the calibration procedure millimeter telescopes generally use a "load" of known temperature that can be placed in the beam path, either inside the cabin (6m dishes) or outside in the ambient air (10m dishes), and the power measured on the load is compared with the corresponding power measurement on the sky. The power measured on the ambient load is

$$P_{load} \;=\; G\{T_{rec} + T_{load}\} \tag{2}$$

where T_{load} is the (Rayeigh–Jeans equivalent of the) physical temperature of the load. The use of these power measurements to determine the telescope calibration is reprised in Appendix 1. For clarity, in our discussion we will ignore the distinction between the receiver sidebands: in general G and τ may be different in the upper and lower sidebands and we have separate equations for both. However, the algebra is much clearer if we ignore this distinction for the exposition.

For the aperture efficiency measurements we use (1), (2) and the power measured while pointing at a suitable planet:

$$P_{src} \;=\; G\{T_{rec} + (1 - e^{-\tau})\eta T_{atm} + (1 - \eta)\,T_{spill} + e^{-\tau}(\varepsilon T_{src} + \eta T_{CMB})\} \tag{3}$$

where T_{src} is the temperature contribution of the target planet diluted over the entire area of the beam, discussed further in the next section. The contribution of the planet is explicitly modified by the telescope "main–beam" aperture efficiency ε as well as the atmospheric opacity. We explicitly assume in (3) that the planet does not fill the primary beam and that the CMB still contributes to the power measured: if this is not the case then one sets $T_{CMB} = 0$ in (3).

For convenience, we now define an effective sky temperature contribution seen by the telescope,

$$T_{sky} \;=\; (1 - e^{-\tau})\eta T_{atm} + (1 - \eta)\,T_{spill} + e^{-\tau}\eta T_{CMB} \tag{4}$$

so that, by analogy with (2), we may write (1) as $P_{sky} = G\{T_{rec} + T_{sky}\}$. We use the common "Y" notation for ratios of the power measurements, e.g.,

$$Y_{load} = \frac{P_{load}}{P_{sky}} \tag{5}$$

We have not yet determined the receiver temperature, but from the ratio $Y_{load} = P_{load}/P_{sky}$ (eqns. 1, 2) we find

$$T_{rec} = \frac{T_{load} - Y_{load}\,T_{sky}}{Y_{load} - 1} \tag{6}$$

Substituting this expression into (1) and (3), with $Y_{src} = P_{src}/P_{sky}$, we derive the following expression for the aperture efficiency:

$$\varepsilon = \frac{Y_{src} - 1}{Y_{load} - 1}\,\frac{T_{load} - T_{sky}}{e^{-\tau}\,T_{src}} = \frac{P_{src} - P_{sky}}{P_{load} - P_{sky}}\,\frac{T_{load} - T_{sky}}{T_{src}}\,e^{\tau} \tag{7}$$

This expression can be simply interpreted as the ratio of the power contributed by the source, $P_{src} - P_{sky}$, to the power expected from multiplying the telescope gain $G = (P_{load} - P_{sky})/(T_{load} - T_{sky})$ by the source temperature contribution T_{src}, corrected for atmospheric absorption of the source with the factor e^{τ}. The aperture efficiency (7) may be evaluated using the 3 power measurements in (1)-(3) together with T_{src}, T_{load} and a value for T_{sky} calculated from measured values of air temperature, pressure and humidity (obtained by the CARMA weather station and available in the monitor data stream) as follows:

- The atmospheric opacity in the 1 mm band is provided by the tipper. No tipper is available at CARMA for the 3 mm band: τ is generally calculated from the expression presented in a note by Dave Woody (summarized in Appendix 2 below). The expression contains a slowly–varying term proportional to the water vapor density, and a pressure- and temperature-dependent approximation to the 119 GHz O_2 line. The value of τ calculated in this way is used in the 3 mm T_{sys} calculation at CARMA. τ at 3 mm can also be measured with a sky dip (see Appendix 3). At the Cedar Flat site at 2000 m altitude, the zenith opacity τ_0 is typically of order 0.03–0.10 in the 3 mm window but 0.2–0.8 in the 1 mm window.

- If $T_{outdoor}$ is the outdoor air temperature near the ground, the effective temperature of the atmosphere at the height of the main atmospheric absorption contribution, T_{atm}, is taken to be $0.94T_{outdoor}$.

- We set $\eta = 0.975$. The value of T_{spill} is not well determined but is not critical here since it only appears multiplied by $1 - \eta$: we use the standard assumption that $T_{spill} = T_{outdoor}$.

- T_{load} is set equal to $T_{outdoor}$ for the OVRO antennas where the absorbing load is outside the electronics cabin, but potentially different for the BIMA antennas where the cal wheel is inside the temperature–controlled cabin, i.e.,

$$T_{load} = \begin{cases} T_{outdoor} & \text{for 10m dishes} \\ T_{cabin} & \text{for 6m dishes} \end{cases} \tag{8}$$

3. Planet temperature contributions

When the target is an extended source such as a planet, we can calculate its temperature contribution T_{src} by diluting the planet disk temperature using the ratio of the area (in solid angle) of the source to the area of the main beam. When the source is a point source, we convert its flux to a diluted temperature. At the present time, planets are invariably modelled as an elliptical disk of constant brightness temperature for calibration purposes, and we will assume circular disks for our discussion. For small sources we thus have

$$T_{src} = \begin{cases} T_{planet} \frac{\Omega_{planet}}{\Omega_A} & \Omega_{planet} \ll \Omega_A \\ \frac{c^2}{2k_B f^2} \frac{S}{1.133\,\theta_{FWHM}^2} & \text{point source of flux } S \end{cases} \tag{9}$$

where Ω_{planet} is the solid angle occupied by the planet ($\pi\theta_{planet}^2/4$, where θ_{planet} is the angular diameter of the planet) and Ω_A is the solid angle for a perfect antenna with an aperture of area $\pi D^2/4$. f is the observing frequency, k_B is the Boltzmann constant and c is the speed of light. Let θ_{FWHM} be the ideal full–width–at–half–maximum of the primary beam of the telescope. For the aperture efficiency measurements the appropriate beam size corresponding to a perfect uniformly and fully illuminated aperture is $\theta_{FWHM} = \lambda/D$, as follows:

$$\theta_{FWHM} = \begin{cases} 59.5'' \, (100/f_{GHz}) & \text{for the 10.4m dishes} \\ 101.4'' \, (100/f_{GHz}) & \text{for the 6.1m dishes} \end{cases} \tag{10}$$

In the case that θ_{planet} is a significant fraction of θ_{FWHM}, we also have to take into account the telescope primary beam response (e.g., Stutzman & Ko 1974). This is modelled by a Gaussian of the form $e^{-\theta^2/2\sigma^2}$ with $\theta_{FWHM} = 2\sqrt{2\ln 2}\,\sigma$. The effective area of such a Gaussian beam pattern is $\pi\theta_{FWHM}^2/4\ln 2 = 1.133\,\theta_{FWHM}^2$. Convolving the Gaussian beam with the planetary disk produces the result that

$$T_{src} = T_{planet} \left(1 - e^{-\ln 2 \frac{\theta_{planet}^2}{\theta_{FWHM}^2}}\right) \tag{11}$$

Similarly, in the case of a point source, the equivalent sky temperature (9) averaged over the area of the beam can be expressed numerically as

$$T_{src} = 1.22 \times 10^6 \frac{S_{Jy}}{f_{GHz}^2 \theta_{FWHM}^2} \tag{12}$$

with S_{Jy} the source flux in Janskies, f_{GHz} the frequency in GHz and θ_{FWHM} measured in arcseconds.

Note that in practice the illumination pattern of the antennas is generally tapered at the edges of the dish in order to reduce spillover, and this increases the effective beam size relative to the "ideal" value used here for aperture efficiency calculations. For interest, Appendix 4 presents measurements of the effective beam size of the CARMA dishes.

Table 1: Single–dish aperture efficiency measurements on Jupiter at 95 GHz

Date/Array	C1	C2	C3	C4	C5	C6	C7	C8	C9	C10	C11	C12	C13	C14	C15
080501/C	0.50	0.47	0.53	0.47	0.46	0.49	0.59	0.53	0.51	0.59	0.48	0.55	0.53	0.42	0.40
080531/C	0.45	0.42	0.46	0.44	0.39	0.42	0.52	0.58	0.57	0.61	0.52	0.51	0.52	0.51	0.57
080601/C	0.50	0.48	0.53	0.49	0.46	0.50	0.57	0.61	0.57	0.65	0.57	0.58	0.58	0.55	0.57
080802/D	0.53	0.51	0.55	0.52	0.48	0.53	0.61	0.59	0.57	0.62	0.59	0.57	0.62	0.58	0.62
080925/E	0.50	0.55	0.55	0.49	0.46	0.52	0.48	0.61	0.52	0.51	0.64	0.59	0.64	0.61	0.46
081002/E	0.47	0.53	0.47	0.49	0.45	0.50	0.49	0.43	0.57	0.36	0.36	0.56	0.08	0.51	0.48
081019/C	0.50	0.53	0.53	0.49	0.46	0.50	0.60	0.60	0.56	0.63	0.61	0.59	0.65	0.58	0.59
081023/C	0.50	0.56		0.50	0.47	0.52	0.63	0.59	0.63	0.68	0.67	0.64	0.65	0.63	0.64
081029/C	0.52	0.56	0.55	0.52	0.50	0.53	0.60	0.61	0.59	0.64	0.62	0.56	0.65	0.61	0.61
081105/C	0.48	0.54	0.54	0.50	0.48	0.50	0.60	0.61	0.61	0.66	0.65	0.61	0.64	0.62	0.66
081113/C	0.45	0.53	0.51	0.46	0.44	0.47	0.56	0.59	0.60	0.64	0.61	0.56	0.63	0.60	0.63
081205/B	0.51	0.54	0.50	0.50	0.49	0.52	0.62	0.61	0.61	0.66	0.66	0.54	0.65	0.62	0.60
081210/B	0.51	0.53	0.52	0.52	0.48	0.53	0.63		0.64	0.67	0.66		0.65	0.61	0.70
081217/B	0.48	0.53	0.49		0.45	0.48	0.64	0.63	0.63		0.71	0.54	0.65	0.61	0.65
090112/A	0.46	0.49	0.49	0.48	0.46	0.50	0.63	0.60	0.62	0.64	0.66	0.68	0.62	0.60	0.64
090114/A	0.46	0.51	0.51	0.51	0.48	0.53	0.60	0.59	0.59	0.61	0.26	0.58	0.61	0.59	0.63
090128/A		0.50	0.51	0.50	0.44	0.48		0.59	0.48	0.57		0.60	0.61	0.53	0.58
090204/A		0.47	0.50	0.49	0.48	0.51	0.47			0.57	0.56	0.59	0.58	0.55	0.60
090218/D	0.48	0.51	0.50	0.54	0.50	0.53	0.59	0.59	0.58	0.60	0.60	0.59		0.57	0.59
090304/D		0.55	0.53	0.49		0.47	0.63	0.42			0.65	0.60	0.64	0.53	0.62
Median	0.50	0.53	0.51	0.50	0.46	0.50	0.60	0.59	0.59	0.63	0.61	0.58	0.63	0.59	0.60

4. Measurements on Jupiter

Data sufficient to carry out the calculation in (7) are acquired (as of June 2008) using the script **Aperture-EfficiencySD.py**. This script is described in more detail in Appendix 5. The power measurements are the Psys values corresponding to each of the 500 MHz spectral bands at the inputs to the CARMA correlator; front–end power measurements in the receiver, with potentially wider bandwidths, were not found to be as stable as the Psys data for this purpose.

Between 2008 May and 2009 February, a significant number of datasets have been acquired using Jupiter as the target; on each date 3 separate measurements were obtained, using each of the three spectral windows. Elevations were generally low (below 25°) due to the low declination of Jupiter. For a given measurement, the 3 spectral windows on a given antenna agreed typically to within 1%. Median efficiencies for each date, calculated using (7), are shown in Table 1. The final row of this table shows the median efficiencies for each

antenna.

The calculations assume a brightness temperature of 179 K for Jupiter at 95 GHz, and diameters (41″ - 45″) obtained from the planetary ephemeris. In these measurements, the 10m antennas generally have efficiencies at 3 mm that are close to 50%, while the 6m dishes are in the 60–65% range, and none of the antennas appear significantly worse that their kin. The results of measurements at 1 mm on Jupiter are shown in Table 2. In both tables anomalies on individual antennas may be found: such anomalies seldom represent true aperture efficiencies, but result from other factors (poor tuning, etc.), and a number of measurements, as are available at 3 mm, are needed in order to recognize clear trends. At present we do not have enough 1 mm measurements to draw strong conclusions. C6 appears consistently to be low (around 33%), and the 10m dishes are significantly less efficient than at 3 mm, as expected, but the variation from one measurement to the next is larger at 1 mm than at 3 mm.

Table 2: Single–dish aperture efficiency measurements at 1 mm

Date/Array	C1	C2	C3	C4	C5	C6	C7	C8	C9	C10	C11	C12	C13	C14	C15
080501/C	0.41	0.14	0.52	0.23	0.39	0.29	0.54	0.53	0.46	0.59	0.50		0.54	0.39	0.49
081023/C	0.39	0.48		0.33	0.40	0.30	0.59	0.57	0.58	0.62	0.55	0.57	0.57	0.64	0.50
081030/C	0.48	0.50	0.49	0.41	0.46	0.35	0.47	0.57	0.58	0.64	0.46	0.53	0.55	0.63	0.38
081205/B	0.38	0.45	0.47	0.38	0.44	0.32	0.61	0.62	0.61	0.65	0.50	0.59	0.57	0.63	0.53
081210/B	0.33	0.30	0.34	0.21	0.37	0.34	0.56		0.53	0.61		0.51	0.55	0.49	0.38
090311/D	0.46	0.40	0.53	0.47	0.56	0.34	0.63	0.57	0.52	0.58	0.45	0.54		0.57	0.50

5. Filled–aperture measurements on the Moon

The Moon is the brightest object available for calibration at millimeter wavelengths because it fills the telescope beam with a source of temperature 100–300 K. However, it also has several drawbacks: its effective temperature varies with position across the disk, and varies dramatically with lunar phase due to solar heating and the time delay required as heat propagates from the lunar surface downwards through the subsurface layers into which millimeter wavelengths penetrate (see Figure 1; Linsky 1973; Mangum 1993; Sandor & Clancy 1995). Another important difference is that because the Moon is so large it fills not only the primary beam, but also any beam sidelobes out to some considerable distance. This is in contrast to observing a smaller object, which occupies only a fraction of the primary beam. Measurements of the power on the Moon are therefore sensitive to the entire forward gain of the dish, rather than just the (smaller) forward gain of the main lobe of the primary beam that is the relevant quantity for aperture efficiency measurements for an interferometer observing a compact source. In the literature the telescope efficiency measured on the Moon, which we will refer to as ε_f, is described as the "forward scattering" efficiency, while the measurement of the efficiency of the main lobe of the primary beam is referred to as the "main beam" efficiency.

In this case the power measured when the telescopes point at the Moon can be represented by the following expression:
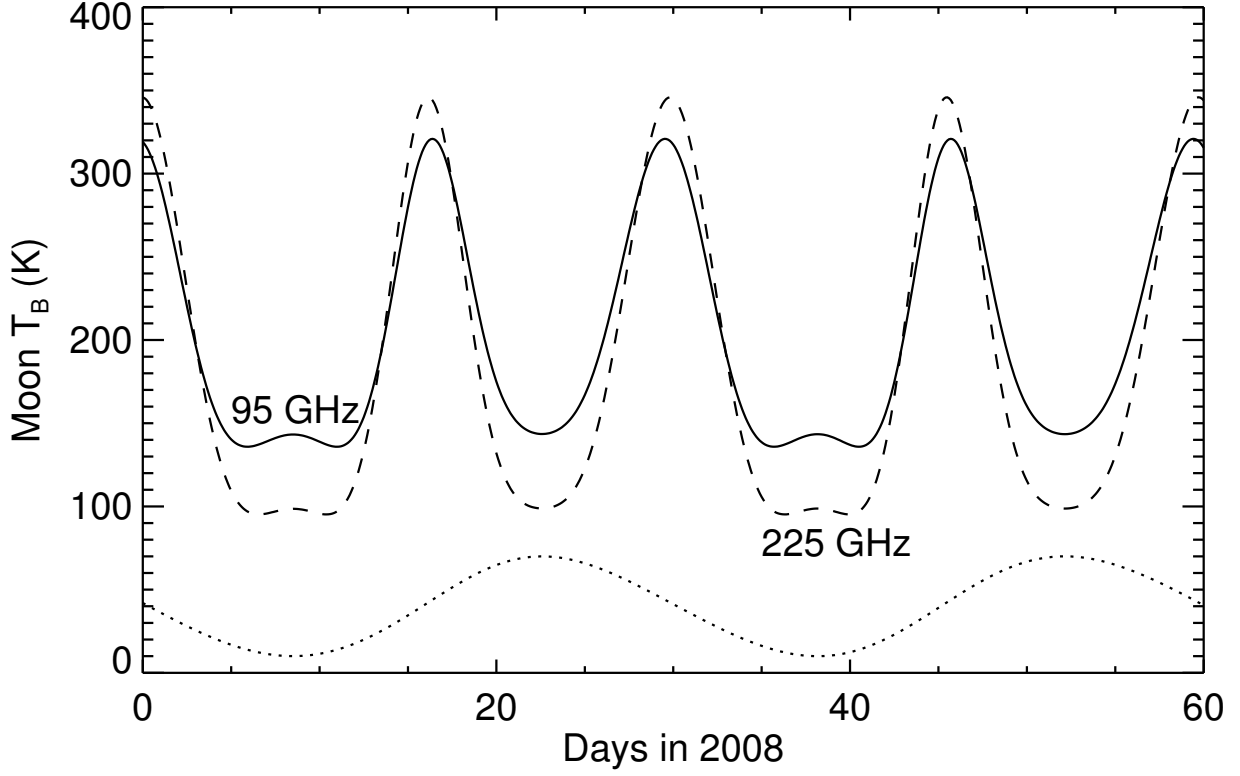
Fig. 1.— Plot of the apparent brightness temperature of the center of the Moon as a function of date in 2008 at 3 mm (solid line) and 1 mm (dashed line) wavelengths. The data are calculated using the formula from Mangum (1993), based on the study by Linsky (1973). The phase of the Moon is plotted as a dotted line at the bottom of the panel: minima in this curve correspond to new moon.

$$P_{moon} = G\{T_{rec} + (1 - e^{-\tau})\eta T_{atm} + (1 - \eta)\, T_{spill} + e^{-\tau}\varepsilon_f T_{moon}\} \qquad (13)$$

The only significant difference from (3) is that the Moon always blocks the CMB entirely, so the CMB no longer contributes to the power on source. Now setting $Y_{Moon} = P_{Moon}/P_{sky}$ and using (1), (2) and (13), after some algebra we find

$$\varepsilon_f = \frac{Y_{Moon} - 1}{Y_{load} - 1} \frac{T_{load} - T_{sky}}{e^{-\tau} T_{Moon}} + \eta \frac{T_{CMB}}{T_{Moon}} \qquad (14)$$

As noted earlier, T_{Moon} is problematic due to its rapid variation in time as direct solar heating moves progressively across the visible disk of the Moon, but at new Moon the disk–center brightness temperature is relatively stable for a few days at minimum values of order 140 K at 95 GHz and 95 K at 225 GHz (see Figure 1). Thus the best time to use the Moon for telescope efficiency measurements is around new Moon.

Table 3 shows the results of single-dish measurements of the Moon on 2008 April 10 (central disk brightness temperature of 222 K from Mangum 1993), April 17 (183 K) and July 31 (close to new moon, 141 K) at 97

GHz. As the table convincingly demonstrates, the absolute values of the efficiencies (frequently in excess of 100%) are not reliable. The variation from one dataset to the next presumably reflects the limitations of the model used for the Moon disk–center brightness temperature. The main feature of these measurements is that all telescopes with good data show very similar efficiencies, with the 6m antennas only slightly better (on average) than the 10m antennas. The similarity across all antennas presumably reflects the fact that the Moon fills all the forward–scattering sidelobes, and any imperfections in main–beam patterns are compensated by the filled sidelobes.

Table 3: Single–dish forward–scattering telescope efficiency measurements on the Moon

Date/Array	C1	C2	C3	C4	C5	C6	C7	C8	C9	C10	C11	C12	C13	C14	C15
080410/C	0.61	0.62	0.61		0.60	0.63	0.68	0.63	0.65	0.68	0.67	0.67	0.65	0.63	
080417/C	1.21	1.23	1.19	1.24	1.15			1.22	1.21	1.28	1.24	1.24	1.22	1.23	1.22
080731/D	1.02	1.02	1.00	1.05	0.97	1.03	1.07	1.04	1.04	1.11	1.08	1.08	1.07	1.08	1.07

Appendix 1: Telescope calibration

As described in CARMA Memo 33 (Woody 2006), we use power measurements on the sky and on an ambient load to determine the telescope system temperature and thus the calibration factors needed to convert the correlator output into calibrated visibilities. At millimeter wavelengths the atmosphere can be a significant issue that needs to be addressed by calibration. A common technique, used by CARMA and previously by BIMA, is to calculate an equivalent temperature of a load *above* the atmosphere that would produce the same power level in the receiver as the ambient load placed in the optical path. This temperature is called T_{cal}, and this method is known as the T_{cal} method. (Note that at some telescopes both hot and cold loads are available, which gives an additional measurement for calibration, but the discussion here only applies to the single–load system appropriate to CARMA.) Recall that the power measured on the sky is, from (1),

$$P_{sky} = G\{T_{rec} + (1 - e^{-\tau})\eta T_{atm} + (1 - \eta)T_{spill} + e^{-\tau}\eta T_{CMB}\}$$

while the power measured on the ambient load is given by (2),

$$P_{load} = G\{T_{rec} + T_{load}\}$$

where, as before, at CARMA T_{load} is the outside air temperature for the 10.4m dishes and the cabin temperature for the 6.1m dishes. We now define T_{cal} to be the temperature of a load placed above the atmosphere that produces the same power measurement in the receiver as the ambient load, i.e., we combine (1) and (2) and set

$$P_{load} = G\{T_{rec} + T_{load}\} = G\{T_{rec} + (1 - e^{-\tau})\eta T_{atm} + (1 - \eta)T_{spill} + e^{-\tau}\eta T_{cal}\} \tag{15}$$

Thus we find that

$$T_{cal} = \frac{T_{load} - (1 - e^{-\tau})\eta T_{atm} - (1 - \eta) T_{spill}}{e^{-\tau}\eta} \tag{16}$$

The contribution of spillover is often ignored, since it is multiplied by the small number $(1 - \eta)$. Note that in (15) we have assumed that the T_{cal} load fills the beam and blocks the CMB; if instead we assume that the T_{cal} load is small, then T_{cal} in (15) is replaced by $T_{cal} + T_{CMB}$ and we do the same thing in (16).

We can now write out an expression for the *system temperature*, defined as the temperature of a load that doubles the output receiver power compared to its value with no load. The system temperature is the critical quantity used to convert the correlation coefficients measured by an interferometer's correlator into visibilities correctly calibrated in Janskies. With $Y_{load} = P_{load}/P_{sky}$ the system temperature becomes (Woody 2006)

$$T_{sys} = \frac{T_{cal}}{Y_{load} - 1} \tag{17}$$

This expression gives the system temperature above the atmosphere since it uses T_{cal}. Optionally, the numerator may be $T_{cal} - T_{CMB}$ if the CMB is always in the beam (not the case when observing the Moon), but since T_{CMB} is of order 1 K and hence is always much less than T_{cal}, we can ignore this subtlety here.

Appendix 2: Opacities from weather data

When the 3 mm opacity at CARMA is not measured with a sky dip but must instead be calculated from weather data (since there appears to be no simple relationship between the 3 mm opacity and the opacity at 225 GHz measured by the tipper), we use a simple approximation to the continuum opacity from Waters (1976) together with a model for the 119 GHz oxygen line due to Dave Woody (described in an 1989 note, and in Andy Beard's note on CARMA flux and T_{sys} calibration):

$$\tau_0 = 0.039 + 0.0090\rho_V + \frac{3.57(P/876)^2(300/T)^{2.5}}{(f_{GHz} - 118.75)^2 + 1.4(P/876)(300/T)^{0.5}} \tag{18}$$

Here P is the pressure in millibars, T is the temperature in Kelvin, f_{GHz} is the frequency in GHz and ρ_V is the "surface absolute humidity" in g m^{-3}. ρ_V is derived from the measured humidity H (as a decimal fraction) as follows: the saturated water vapor pressure for a given temperature T is

$$P_{H2Osat} = 6.11\left(\frac{T}{273}\right)^{-5.3} e^{25.2\frac{T-273}{T}} \tag{19}$$

Then the partial vapor pressure is just $P_{H2O} = H P_{H2Osat}$ and $\rho_V = 217 P_{H2O}/T$, i.e.,

$$\rho_V = 1325 H \left(\frac{T}{273}\right)^{-6.3} e^{25.2 \frac{T-273}{T}} \tag{20}$$

Note that τ_0 is the zenith opacity, i.e. looking straight upwards (90° elevation). At any other elevation El the opacity is proportional to the air mass appropriate to that line of sight:

$$\tau = \tau_0 \sec(El) \tag{21}$$

In the 1 mm band, the τ_0 measurement reported by the tipper should be used when available. Initially the tipper was controlled by a laptop independent of the rest of the CARMA control system and the tipper data were not available in the monitor data stream. The tipper measurements were however to be found on the plots used at CARMA to assess the viability of 1 mm observations, and they are stored in the directory /array/rt/TipperData. The monitor–stream variable is "OpacityMonitor.tau225", but at the time of writing (2009 February) this variable is zeroed out. Instead the monitor data stream reports the zenith value τ_{225} derived for 225 GHz from the precipitable water vapor measurement according to the following approximation:

$$\tau_{225} \approx 0.06 \, \text{precip}_{mm} + 0.005 \tag{22}$$

where precip_{mm} is the precipitable water column in millimeters reported by the weather station. Comparison of this formula with the tipper data suggests that it is correct to within about 20%. This is the value used in (16) to calculate the system temperature.

Appendix 3: Sky dips

In order to measure the zenith opacity τ_0 in practice, one can carry out a "sky dip": the power on the sky, P_{sky}, is measured at a number of different elevations, El. By (1),

$$P_{sky}(El) = G\{T_{rec} + \eta \, T_{atm} + (1 - \eta) \, T_{spill} - \eta \, (T_{atm} - T_{CMB}) e^{-\tau_0 \sec(El)}\} \tag{23}$$

Assuming that we have also measured the power on the ambient load given by (2), we may fit the measured Y–factor P_{load}/P_{sky} as a function of air mass $AM = 1/\sin(El)$ and the receiver temperature ratio $R = T_{rec}/T_{atm}$ and determine both τ_0 and T_{rec}:

$$Y(AM) = \frac{P_{load}}{P_{sky}(AM)} = \frac{R + T_{load}/T_{atm}}{R + \eta \, (1 - e^{-\tau_0 AM}) + (1 - \eta) \, T_{spill}/T_{atm} + \eta \, e^{-\tau_0 AM} \, T_{CMB}/T_{atm}} \tag{24}$$

As noted earlier, the relevant efficiency η that appears in this expression is not the main–beam efficiency that is the principal subject of this memo, but rather the spillover or coupling efficiency. η is taken to be close to unity in the dip analysis: at the Arizona 12m telescope $\eta = 1$ is used, while at CARMA we set $\eta = 0.975$.
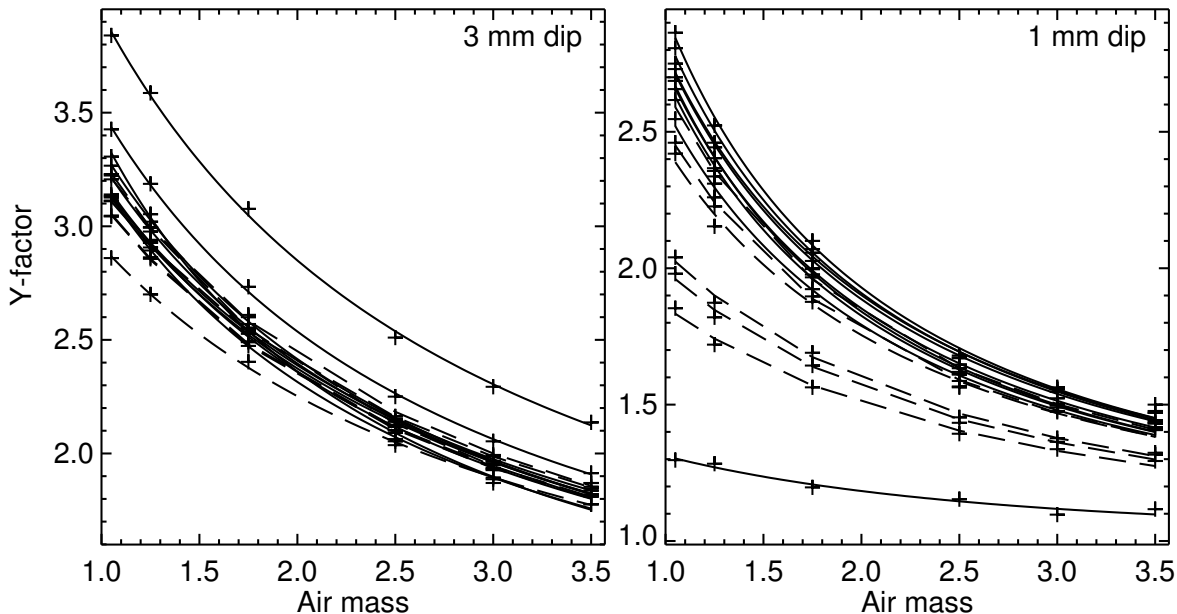
Fig. 2.— Plot of the "Y–factor" (ratio of ambient–load power to sky power) versus air mass for measurements at 3 mm (113 GHz, left panel) and 1 mm (222 GHz, right panel) for each of the 15 CARMA antennas. The measured values (averaged over the three observing bands) at each of 6 different air mass values are plotted with cross symbols, and the best–fit shape of (25) is shown by a line (dashed for the 10.4m antennas, solid for the 6.1m antennas).

The standard single–load calibration approach available at CARMA does not generally provide enough data to determine unambiguously all the variables (τ_0, T_{rec}, η, T_{spill}) in this equation.[1] In practice the assumption that T_{spill} does not depend on elevation is not correct: the dish elevation influences how much of the spillover is warm ground and how much is cold sky, so adopting a constant value for T_{spill} is not strictly appropriate. However, in practice T_{spill} appears only in the denominator multiplied by a small number, and usually does not make a large contribution to the measured power, so the assumption of constant T_{spill} does not significantly bias the results.

In the limit that $\tau_0 AM \ll 1$ and ignoring T_{CMB}/T_{atm}, $(1 - \eta) \ll 1$, we can write

$$Y(AM) = \frac{R + T_{load}/T_{atm}}{R + \tau_0 AM}$$

A plot of Y versus AM should therefore show a simple hyperbolic shape. The necessary data are acquired at CARMA using the script **dip1.py**. We fit equation (24) for τ_0 and T_{rec} for each antenna separately with the assumptions described above ($\eta = 0.975$, $T_{spill} = T_{outdoor}$) using an IDL routine that carries out a

---

[1]James Lamb uses an additional liquid nitrogen load for spillover measurements on the CARMA dishes, but this presently is a two–person operation that is carried out one telescope at a time and requires taking the dish out of the array.

Levenberg-Marquardt least-squares minimization of (24) (the routine optionally allows T_{spill} to be included in the fit, or allows τ_0 to be held fixed). An example of such data (acquired on 2008 June 15 at 113.2 GHz and 222.0 GHz) and the corresponding fits is shown in Figure 2, with the results of the fits given in Table 4. Each antenna can be well fit by the functional form (24) and the resulting values of τ_0 agree surprisingly well between the 15 antennas even though the shapes of the curves, and the corresponding T_{rec} values, vary considerably (C13 is clearly anomalous at 1 mm, with an anomalously poor T_{rec}).

Table 4: Sky–dip measurements of opacity and receiver temperature on 2008 June 15

Antenna	3 mm τ_0	1 mm τ_0	3 mm T_{rec}	1 mm T_{rec}
C1	0.19	0.37	85	64
C2	0.19	0.37	71	165
C3	0.19	0.37	64	43
C4	0.21	0.38	57	115
C5	0.18	0.38	72	54
C6	0.19	0.38	72	129
C7	0.19	0.37	56	35
C8	0.15	0.35	49	34
C9	0.20	0.36	63	38
C10	0.20	0.35	60	41
C11	0.19	0.38	68	36
C12	0.21	0.36	59	29
C13	0.19	0.52	54	498
C14	0.19	0.37	67	47
C15	0.23	0.37	45	39

The weather data predict opacities (as described in Appendix 2) of order 0.18 at 3 mm (where the two sidebands were at 111 and 115 GHz, so they saw very different opacities) and 0.3-0.4 at 225 GHz during the data acquisition, while the 230 GHz tipper reported a zenith opacity in the range 0.32 to 0.35, in quite good agreement with our 1 mm dip value. Figure 3 shows a comparison of measured sky–dip opacities with the values derived from the weather data as described in the previous section for a number of measurements in 2008/2009. While the 1 mm formula appears to work quite well, there is a clear problem with the 3 mm formula (18): it predicts very little variation in opacity at frequencies below 110 GHz where the oxygen line has no significant contribution. Opacities at 100 GHz are almost always predicted to be around 0.05 from the weather data, being dominated by the constant 0.04 term in (18), while the 3mm dip measurements show much more variation in reality. From (16), the system temperature measurement at low opacities is proportional to $1 + \tau$, so, e.g., use of the value $\tau = 0.05$ in calculating T_{sys} when the true value should be $\tau = 0.10$ results in a 5% underestimate of T_{sys}.
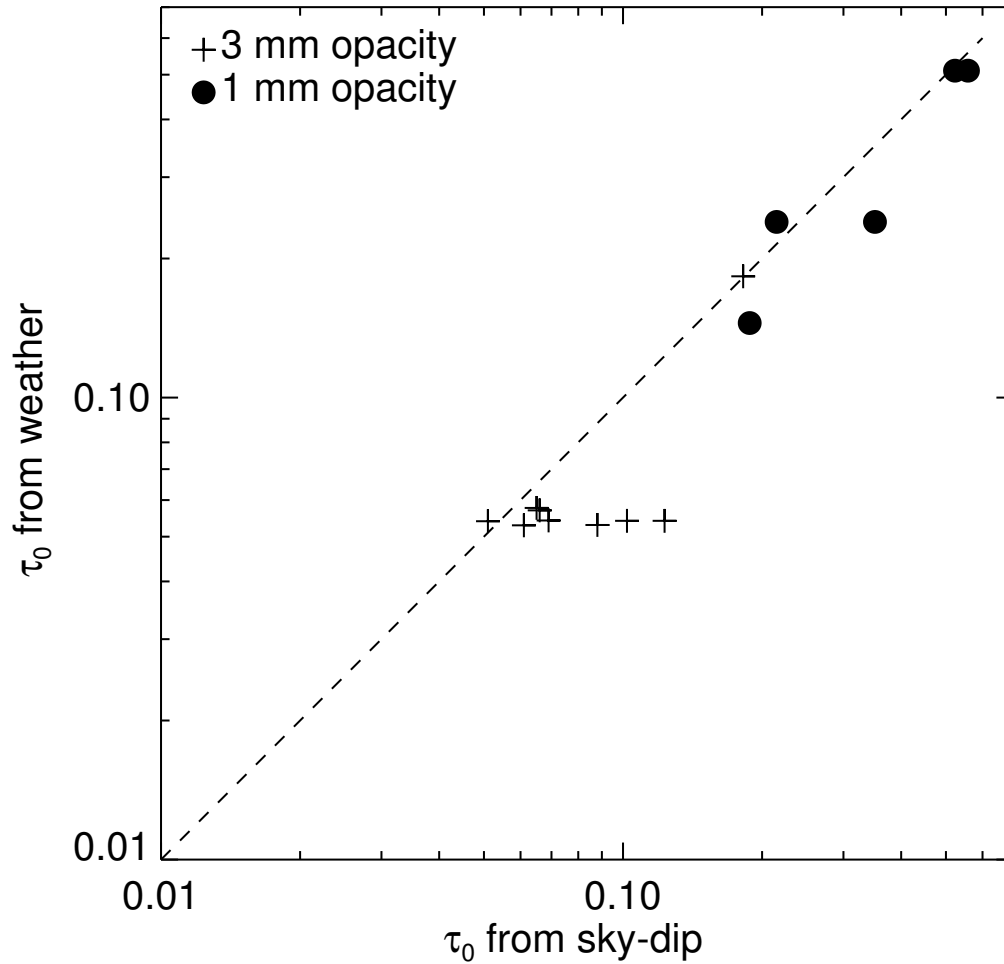
Fig. 3.— A comparison of measurements of zenith opacity from sky dips with the corresponding values predicted from the weather data using equations (18) and (22) at 3 mm (plus symbols) and 1 mm (dot symbols), respectively.

To fit dip data at CARMA, follow the instructions in the file *tau_dip_instructions.txt*; alternatively, there is a one-step IDL routine as follows, e.g.,

```
cd /array/rt/Dips
idl
IDL> fit_dip,'2008may31.dip1_tsys.dat',/output
```

Since the data for each fit (each of 3 bands on each of 15 antennas) is independent, consistency between antennas indicates a good result. We generally find this to be the case with CARMA dip data.

Appendix 4: Primary beam sizes

As discussed by Baars (2003), the actual size of an antenna primary beam depends on the way in which the dish surface illuminates the subreflector and then the feed horn. In practice it is usually easier to think about this in reverse order with the feed horn as a radiator that illuminates the subreflector and in turn the dish surface. The illumination pattern (which in theory is a Bessel function for a uniform circular aperture, not a Gaussian function) can be controlled by the design of the feed horn and subreflector, and is often tapered at the edges of the dish in order to reduce spillover effects at the edge of the primary beam, with the effect that the full dish aperture is not being used and the primary beam size is slightly larger than the canonical value for uniform illumination of the dish (no tapering), $\theta_{FWHM} = \lambda/D$, where λ is the wavelength and D the dish diameter (Baars 2003, finds $1.02\,\lambda/D$ in practice for uniform illumination out to the edge of the dish). For a typical Gaussian taper with an 11 dB reduction in sensitivity at the edge of the illumination pattern compared to the center of the dish, $\theta_{FWHM} = 1.22\lambda/D$ (which also happens to be the angular size of the first null in the Bessel function pattern of a uniformly illuminated dish). Most real dishes lie somewhere between these two limits, e.g., Lugten (1995) reports that $\theta_{FWHM} = 1.14\lambda/D$ for the antenna power pattern in his analysis of the performance of the $D = 6.1$m BIMA antennas. For the CARMA dishes, different illumination patterns give the beam sizes (at 100 GHz) reported in Table 5.

Table 5: Theoretical CARMA antenna primary beam sizes (FWHM) at 100 GHz

	10.4m dishes	6.1m dishes
λ/D	59.5″	101.4″
$1.14\lambda/D$	67.8″	115.6″
$1.22\lambda/D$	72.6″	123.8″

As part of the radio pointing procedure at CARMA, Gaussian fits are made to the widths of the primary beams in order to exclude bad data, so the radio pointing data contain a large number of actual fits of the amplitude (not the power) FWHM. Note that in practice a Gaussian is not always a good representation of the beam pattern (Corder & Wright 2006; Wright & Corder 2008). We have gone through recent data and using close to 500 "good" measurements per antenna, we find that the mean primary beam sizes (geometric mean of azimuth and elevation axis widths, converted to the power FWHM assuming that it is the amplitude FWHM divided by $\sqrt{2}$) at 100 GHz are as shown in Table 6. The results in this table correspond to $1.10\lambda/D$ for the 10.4m dishes and $1.07\lambda/D$ for the 6.1m dishes.

Appendix 5: The ApertureEfficiencySD script

In this appendix we describe the script for acquiring single–dish aperture efficiency data (as of July 2008). The script is invoked as follows: in sac (the python subarray controller), type, e.g.,

Table 6: Measured CARMA antenna primary beam sizes (FWHM) at 100 GHz

Antenna	Median (″)	Mean (″)	St. dev. (″)
1	65.5	65.7	± 2.4
2	65.0	65.4	± 2.5
3	63.4	63.7	± 2.4
4	66.7	67.1	± 2.7
5	65.2	65.4	± 1.7
6	66.6	66.8	± 2.2
7	106.6	106.8	± 3.0
8	107.9	108.3	± 3.6
9	109.1	109.5	± 3.2
10	108.9	109.3	± 2.9
11	110.0	110.7	± 3.8
12	108.9	109.0	± 3.2
13	108.5	108.8	± 3.0
14	108.4	108.7	± 3.4
15	108.5	108.7	± 3.6

```
   import ApertureEfficiencySD as SD
   SD.CalculateApertureEff(planet='jupiter',tuning_frequency='3mm', \
      pointing_source='1924-292')
or
   SD.CalculateApertureEff(planet='moon',tuning_frequency='3mm', \
      performPointing=False,myoffset=20.)
```

The keywords should be fairly self–explanatory: reference pointing is not necessary on the Moon since it is so large. The offset on the Moon (in arcminutes) is for the sky power measurement: it needs to be large enough to move off the planet (defaults to 5′).

The script carries out the following actions:

- Tunes to "3 mm" (IF at 95 GHz) or "1 mm" (IF at 223.0 GHz).

- Carries out reference pointing (if requested; highly desirable for any source except the Moon). Generally a nearby quasar should be used, since pointing on large planets is not reliable.

- Reads the weather data necessary for the load temperatures and to calculate atmospheric opacity (Drive.Weather.ambientTemp at each active 10m antenna, BimaSpecific.CalPlate.tempAmb at each

active 6m antenna, Weather.Tau225, PhaseMonitor.skyRMS, Weather.DewPointSensor.humidity, Weather.pressure, Weather.waterDensity, Weather.precipWater) from the monitor stream.

- The physical parameters of the planet (brightness temperature, size), which are extracted from the planetary ephemeris and loaded into the monitor data when the source name is set, are read (Control.-Subarray*n*.planetTemperature, Control.Subarray*n*.planetMajorAxis, Control.Subarray*n*.planetMinorAxis) and recorded.

- If desired (checkPointing=True, not the default) carries out an interferometer measurement on the planet in a cross pattern to check that the pointing is good (generally not needed).

- Offsets in azimuth from the planet, then the ambient load is placed into the beam path and the power on the load is measured. Each time the power is measured, the following is done: the elevation is recorded, T_{sys} is determined for each antenna and band (monitor point SlPipeline.Input*n*.Band*m*.-Tsys.Dsb), the P_{sys} power values at the inputs to the correlator (Sldc.Band*m*.Input*n*.psys) are recorded, and for comparison the front–end power levels (*n*.AntennaIfContainer.AntennaIF.ifOutTotalPower), which sample a wider bandwidth but are less stable than the P_{sys} powers and hence are not used for the final analysis, may be recorded. Each of these measurements may be sampled up to 20 times, but tests indicate that a single P_{sys} power measurement is sufficiently repeatable.

- The load is removed from the beam path and the power P_{sky} is measured in the sky position.

- The antennas are moved back to the source, the ambient load is placed in the beam path and the power is measured.

- The load is removed from the beam path and the power P_{src} is measured on the source.

- This cycle is repeated 3 times.

- A sky dip is carried out at the observing frequency to measure the sky opacity (unless skyDip=False).

The output data files are written to the directory /array/rt/apertureEff/singleDish. There are then two paths for the final calculation of aperture efficiency: a python script, and an IDL routine. The python analysis routine SingleDishEfficiency.py is the result of the conversion by Brian Prager of an Excel spreadsheet of Ashley Zauderer and can be invoked as follows, e.g.

```
cd /array/rt/apertureEff/singleDish
Preprocess_Data.csh 3mmfreq2008mmmdd.SD.planet.dat
cd 3mmfreq2008mmmdd.planet
../SingleDishEfficiency.py A=43.81 Tau225=.436 In=output.txt TPlanet=179 \
   IntTime=.5 BandWid=1.5 Date=06-01-2008 Tout=282.75 Elevat=30.2 Phase=372 \
   Freq=97.15 Tau=.09 Planet=Jupiter Full=0 Out=Efficiencies.dat \
   Stat=Stats.dat
```

Presently the planet data and atmospheric data have to be supplied as keywords. A future version will avoid this need. To use the IDL version, in the same directory run the routine **sd_to_eff** with the data file name as an argument:

```
cd /array/rt/apertureEff/singleDish
idl
IDL> sd_to_eff,'3mmfreq2008aug02.SD.jupiter.dat',/output
IDL> exit
```

With the `/output` option the results are written to a file in the Results subdirectory; optionally, the zenith opacity measured by the sky dip can be used in place of the weather value by supplying it as a keyword (`tau=...`).

Acknowledgements

REFERENCES

Baars, J. W. M. 2003, ALMA Memo 456: Characteristics of a reflector antenna (NRAO/ESO)

Corder, S. & Wright, M. C. H. 2006, CARMA Memo 36

Folkers, T. W. 2004, Users Manual for the ARO 12m Millimeter-Wave Telescope (Tucson: Arizona Radio Observatory)

Kramer, C. 2005, Spatial response framework document of the HIFI/Herschel Calibration Group (KOSMA/Uni. Köln)

Kutner, M. L. & Ulich, B. L. 1981, Astrophys. J., 250, 341

Linsky, J. L. 1973, Astrophys. J. Supp., 25, 163

Lugten, J. B. 1995, BIMA Memo 39: Optical Design and Performance of the BIMA Interferometer

Mangum, J. 2002, ALMA Memo 434: Load calibration at millimeter and submillimeter wavelengths (NRAO/ESO)

Mangum, J. G. 1993, Publ. Astron. Soc. Pacific, 105, 117

Moreno, R. & Guilloteau, S. 2002, ALMA Memo 372: An amplitude calibration strategy for ALMA (NRAO/ESO)

Plambeck, R. L. 2000, ALMA Memo Series, 321

Sandor, B. J. & Clancy, R. T. 1995, Icarus, 115, 387

Serabyn, E., Weisstein, E. W., Lis, D. C., & Pardo, J. R. 1998, Applied Optics, 37, 2185

Stutzman, W. L. & Ko, H. C. 1974, IEEE Transactions on Antennas and Propagation, 22, 493

Ulich, B. L. & Haas, R. W. 1976, Astrophys. J. Supp., 30, 247

Waters, J. W. 1976, in Methods of Experimental Physics, Vol. 12B, ed. M. L. Meeks (New York: Academic Press), 142

Woody, D. P. 2006, CARMA Memo 33

Wright, M. C. H. & Corder, S. 2008, CARMA Memo 43